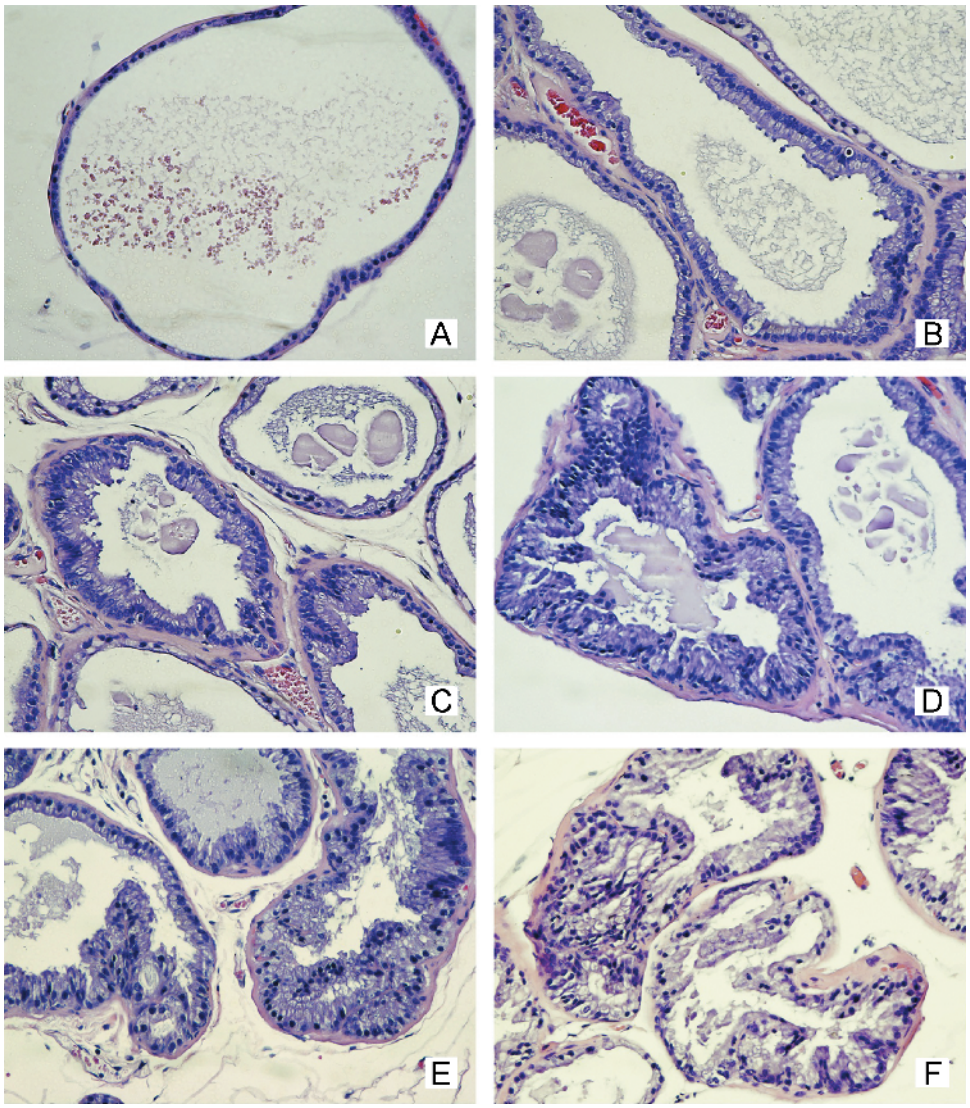

Figure W1. H&E-stained sections of the ventral prostate from $ARR_2Pb.Stat3C$ mice at 12 months. Areas of normal tissue, hyperplasia, and PIN lesions are shown. (A and B) Ventral prostate showing a single stratum of luminal epithelial cells with normal flat morphology for quiescent glands (A) and typical cells with cylindrical shape in an active epithelium (B). (C and D) Ventral prostate from a 12-month-old mouse showing luminal epithelial hyperplasia without cellular atypia (C) and with cellular atypia (D). The hyperplasia was characterized by an increase in epithelial tufting but otherwise the appearance of the cells was relatively normal. (E and F) PIN lesions were characterized by cell enlargement, karyomegaly, karyocytomegaly, nuclear atypia with apical localization, chromatin condensation, and the presence of one or more prominent nucleoli. Also, a cribriform growth pattern, as well as the formation of many small intraluminal glands, was noted. Magnifications, $\times 10$.

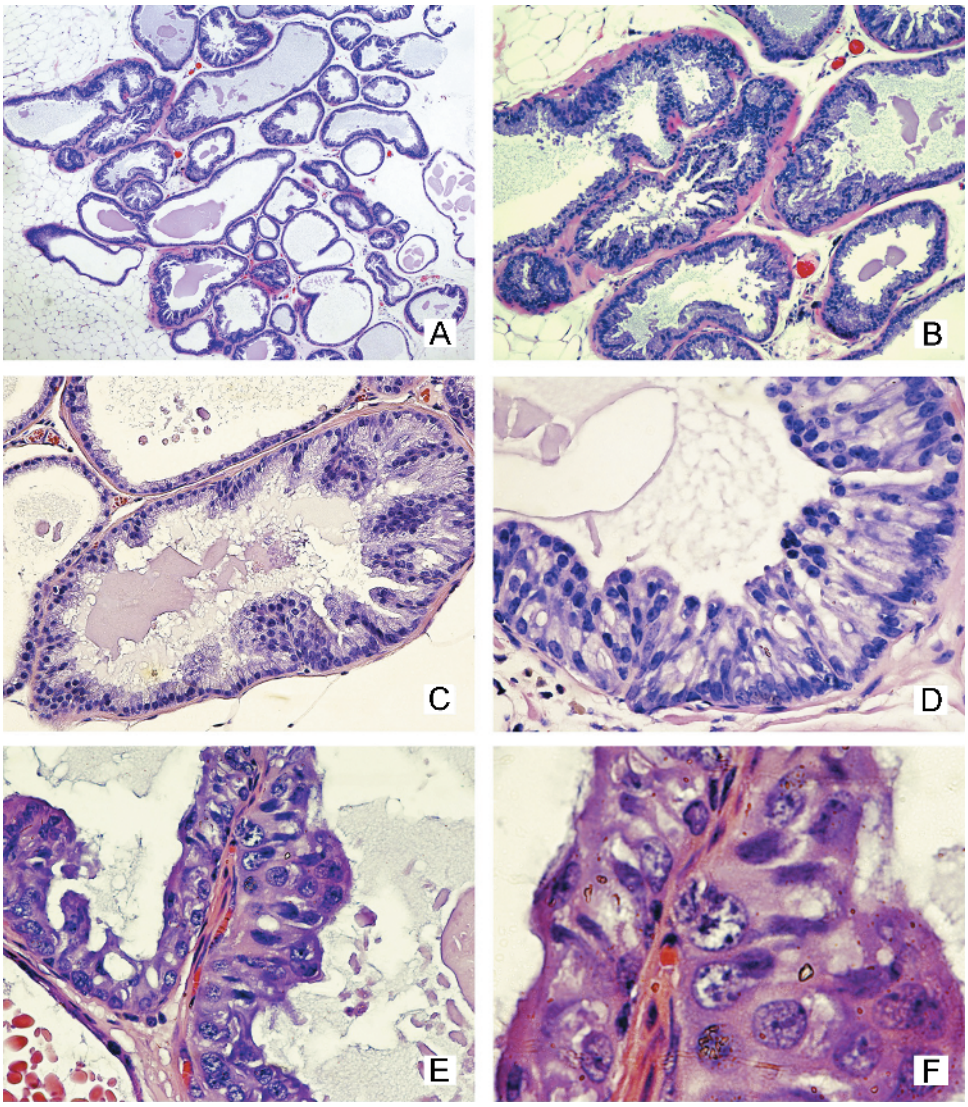

Figure W2. Additional H&E-stained sections of lesions in the ventral prostate from ARR_2Pb.Stat3C mice. (A and B) Areas of the ventral prostate with mixed normal tissue and PINs with fusiform and cribriform patterns (4×). (C and D) The ×10 and ×20 magnifications of a PIN lesion. Note that the nucleus in cells of this PIN lesion are adopting an apical position compared with a more basal position in the normal cells. (E and F) Higher magnification (×40 and ×100) of the PIN lesions in the VP. This section shows the variety of shapes of the dysplastic nuclei and cells. Cells also presented with karyocytomegaly and an increase in number and size of the nucleolus. Note the difference in the sizes of the nucleolus among cells as well as chromatin condensation and nuclear atypia.

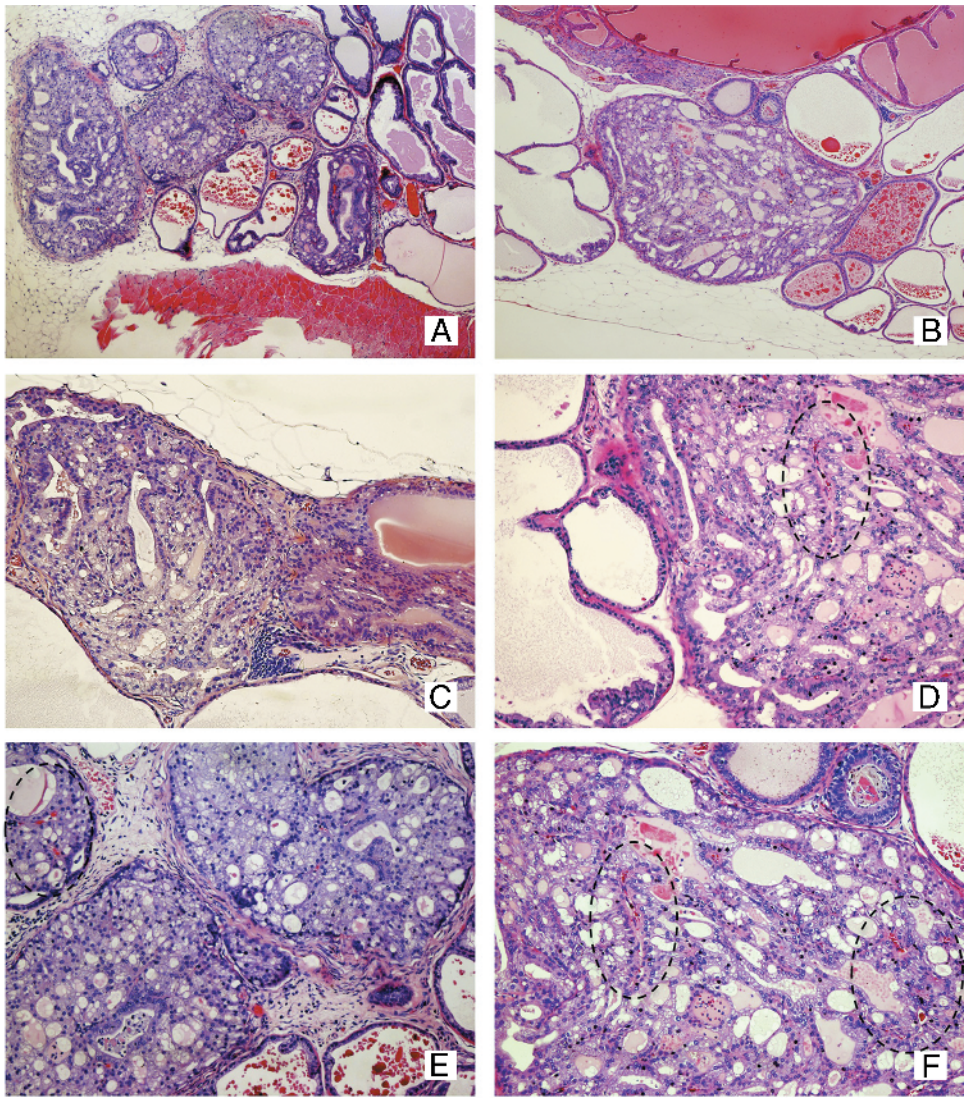

Figure W3. Additional examples of invasive adenocarcinomas in the ventral prostate of double transgenic ($ARR_2Pb.Stat3C \times PTEN^{+/-}$) mice. (A and B) Adenocarcinomas from the ventral prostate of a 12-month-old $ARR_2Pb.Stat3C \times PTEN^{+/-}$ mouse. Note the widespread local invasion of moderate- to well-differentiated tumor cells (×4). (C–F) Higher magnifications (×10) of adenocarcinomas from the ventral. Circles in panels D, E, and F show areas of neovascularization inside of the neoplastic gland.

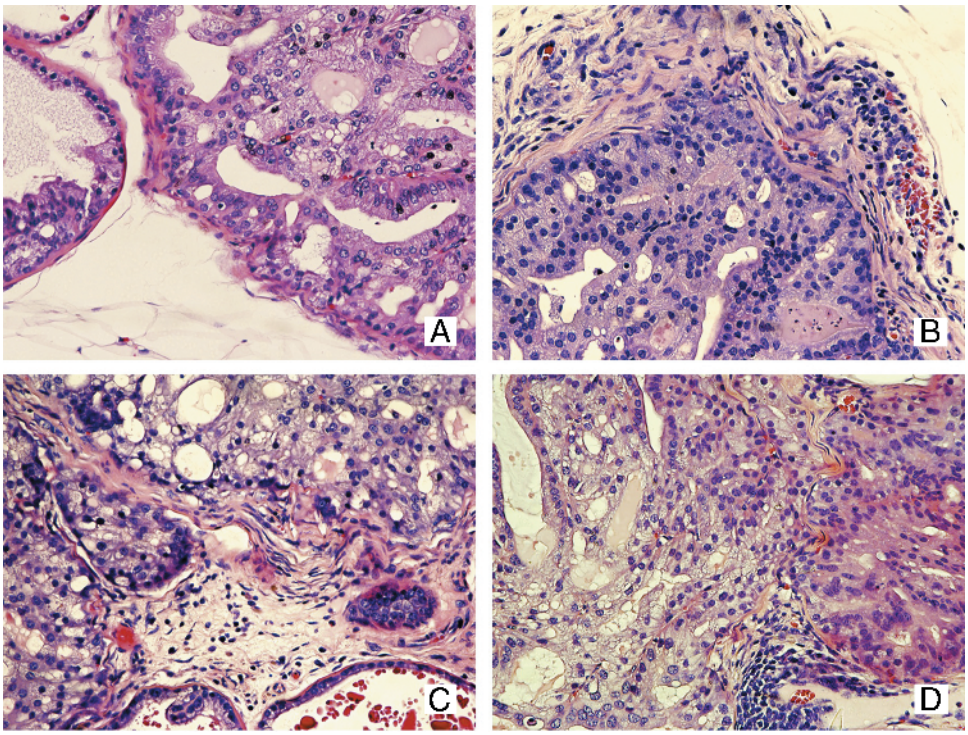

Figure W4. (A–D) Additional examples (larger magnification) of neoplastic glands with clear membrane disruption and stromal invasion. Note also the formation of small intraluminal glands.

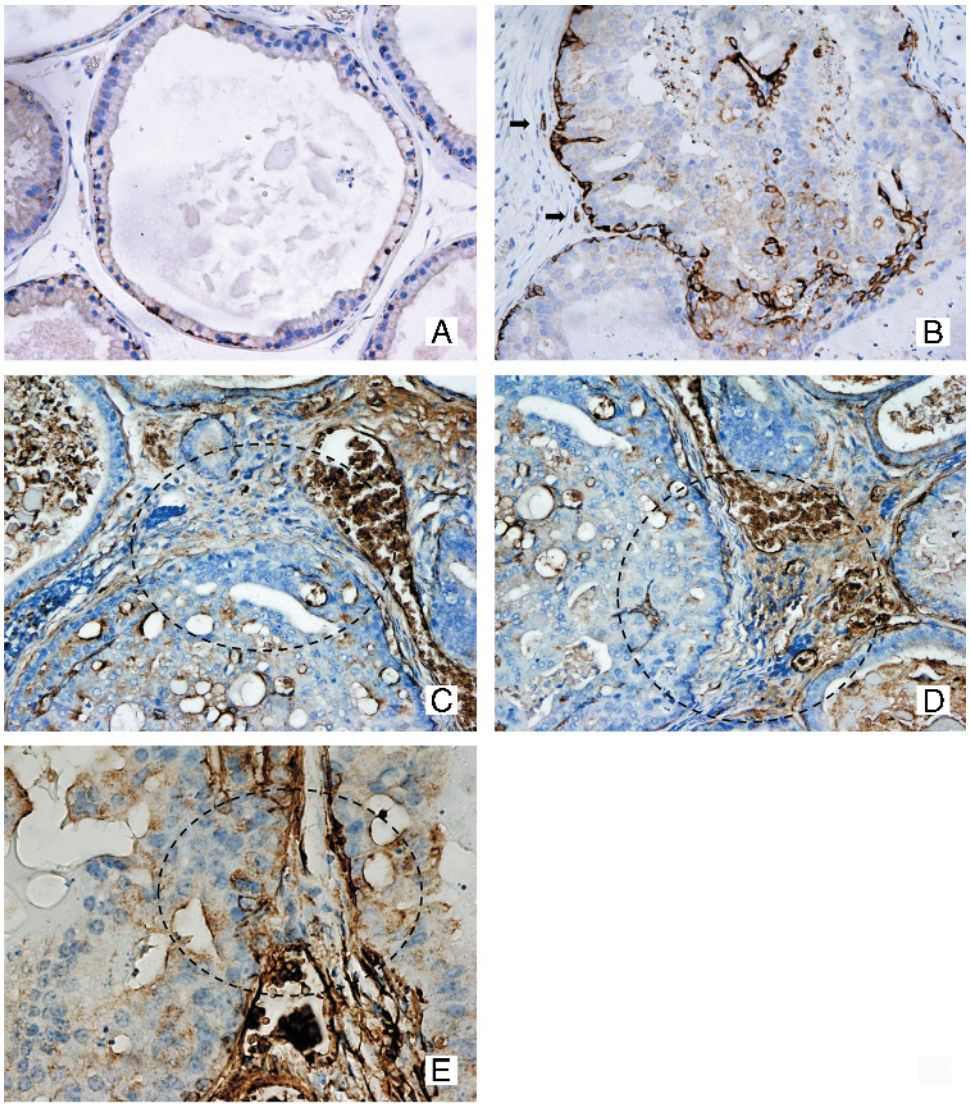

Figure W5. IHC staining for K14 and laminin in tissue from the ventral prostate of the $ARR_2Pb.Stat3C \times PTEN^{+/-}$ mice. (A) K14 staining of a normal gland (WT mouse) denoting a basal cell staining. (B) K14 staining of an adenocarcinoma from an $ARR_2Pb.Stat3C \times PTEN^{+/-}$ mouse. K14 was largely expressed in basal cells and in cells infiltrating the lumen of the neoplastic gland. In addition, K14 was expressed in some cells found in the stroma (arrows). (C–E) Laminin staining: pictures show a clear membrane disruption and adjacent invasion in the affected glands (circles).

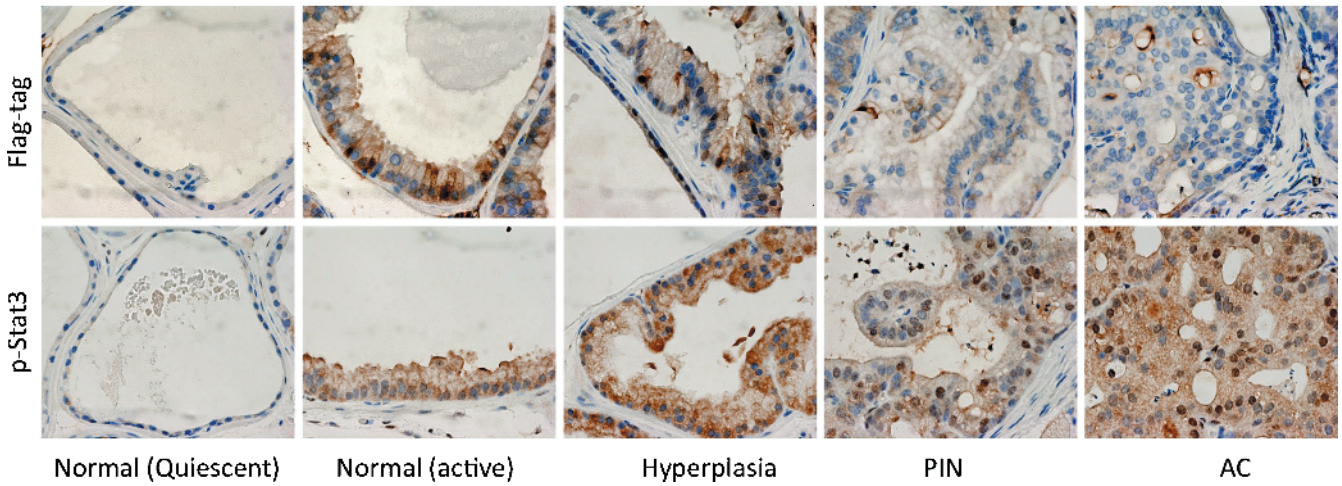

Figure W6. Composite picture showing IHC staining for the transgene (Stat3C) using antibodies to the Flag-tag and for phospho-Stat3 (using antibodies for phospho-Tyr^{705}) in normal glands (both quiescent and active), hyperplasia, PIN, and ACs from ventral prostate of the $ARR_2Pb.Stat3C \times PTEN^{+/-}$ mice. Stat3C was expressed in the normal (active) glands and hyperplastic glands from the ventral prostate of double transgenic mice. Staining was seen in both the cytoplasm and nucleus. Transgene expression (both cytoplasmic and nuclear) was reduced in both PIN and ACs. In contrast, phospho-Stat3 (Tyr^{705}) was primarily cytoplasmic in normal (active) and hyperplastic glands with strong nuclear staining in PIN and ACs.

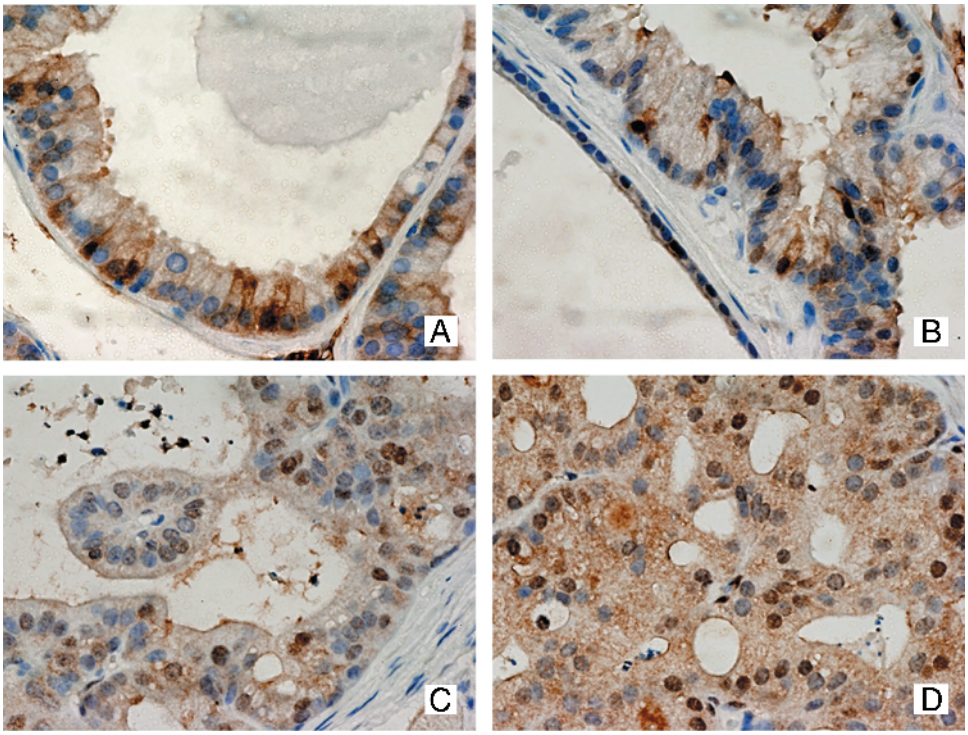

Figure W7. Higher magnification (×40) from the previous composite images of Flag-tag (Stat3C) staining in normal (active) and hyperplastic glands (A and B) and nuclear phospho-Stat3 staining in PIN and adenocarcinomas (C and D).

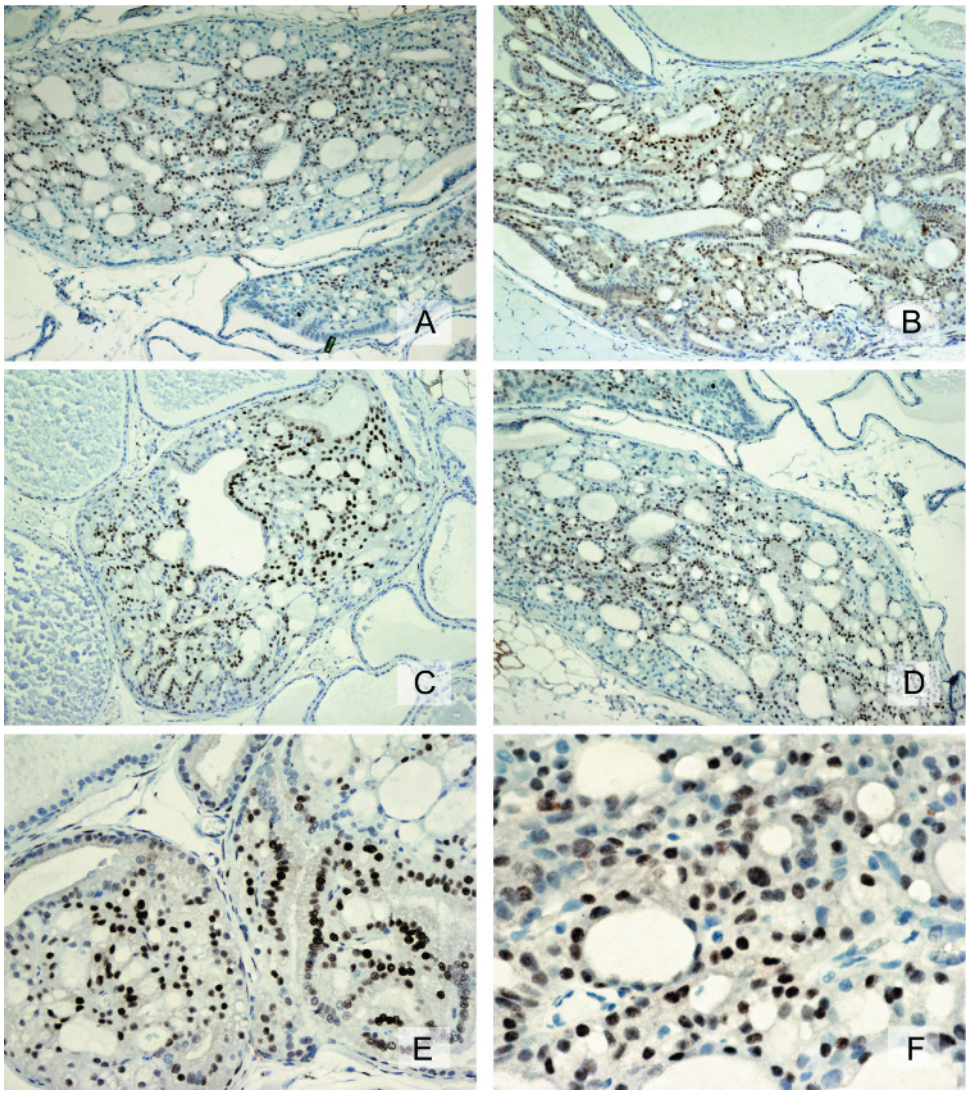

Figure W8. Additional IHC analyses of VP from 6- and 12-month-old $ARR_2Pb.Stat3C \times PTEN^{+/-}$ transgenic mice ($n = 5$) for phospho-NF-κB (p65). Strong nuclear staining was observed in 100% (5/5 samples) of the adenocarcinomas from the double transgenic mice. (A–D) Samples from four different mice (magnification, ×10). (E) Sample from another double transgenic mouse (magnification, ×20). (F) Higher magnification (magnification, ×40) of the same sample shown in panel D.